Molecular Catalysts for Water Oxidation

Masayuki Yagi and Masao Kaneko*

Faculty of Education and Human Sciences, Niigata University, Niigata 950-2181, Japan, and Faculty of Science, Ibaraki University, Mito 310-8512, Japan

Contents

I. Introduction

Water oxidation to evolve dioxygen (O_2) (eq 1) catalyzed at the oxygen-evolving center (OEC) in photosynthesis is one of the most important and fundamental chemical processes in nature.[1−12] Electrons are provided to the reaction center of photosystem II and ultimately appear as reduced carbon products by this process, which is the origin of all biological activities.

$$2H_2O \xrightarrow{\text{Molecular catalyst}} O_2 + 4H^+ + 4e^- \qquad (1)$$
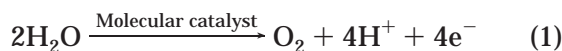
It has been established that an oxo-bridged tetramanganese aggregate is involved in the photosynthetic OEC protein.[13,14] Manganese complexes have been extensively studied as artificial OEC models for providing structural and mechanistic clues to evaluate O_2 evolution from water taking place at the photosynthetic OEC.[7−9] Manchanda and Brudvig et al. summarized the preparation, structures, and redox properties of manganese clusters as structural modes of the photosynthetic OEC.[7] Law and Pecoraro summarized aspects and spectroscopic features of mono- and multinuclear manganese complexes as models for the multinuclear manganese-containing enzymes.[9] Ruettinger and Dismukes reviewed the thermodynamics and kinetics of water oxidation at the photosynthetic OEC and discussed synthetic water oxidation catalysts to provide mechanistic insight into photosynthetic water oxidation.[6]

It is important to establish an artificial OEC model not only for understanding and simulating the photosynthetic OEC, but also to construct artificial photosynthesis, which is attracting a great deal of interest to convert solar energy into fuels.[2−5,10−12] The available water oxidation catalysts capable of evolving O_2 from water are very few in number. Herein we will review molecular aspects and activities of water oxidation catalysts to provide concepts for designing an active and stable OEC model system. The present review focuses on the recent literature after 1996. Other previous reviews are available for the works before 1996.[5,6] First, photosynthetic OEC will be reviewed to provide an understanding of the structure and catalytic mechanism of photosynthesis in section II. Homogeneous catalysis by transition-metal complexes, especially by Mn and Ru, will be summarized in section III, followed by molecular aspects and analyses of catalytic activities in heterogeneous catalysis including photocatalysts for O_2 evolution in section IV. Finally, approaches to establish an artificial photosystem II (PS II) model where visible light induces water oxidation to evolve O_2 will be described in section V.

II. Photosynthetic Oxygen-Evolving Center

By light absorption of a chlorophyll aggregate P_{680} in photosystem II (PS II), electron transfer occurs from the excited P_{680} to a primary electron acceptor pheophytin and subsequently to two quinones, forming P_{680}^+ radical cation. The OEC involved in PS II serves as an electron donor to P_{680}^+, and this electron transfer is mediated by a Tyr_Z residue. The OEC contains a unique oxo-bridged manganese aggregate responsible for the catalytic water oxidation to evolve O_2. The current model of OEC involves five intermediate states from S_0 to S_4 (Scheme 1, the so-called Kok cycle).[15]

In the last three decades, numerous works have been published on the chemical and electronic structures as well as oxidation state of the intermediate of the manganese cluster, including a water oxidation mechanism and the role of cofactors of Tyr_Z, His residues, and Cl^- and Ca^{2+} ions in the OEC.[13−35] Despite these works using various biophysical methods to investigate the OEC, its complete structure and mechanism still remain unsolved. A brief summary of water oxidation by the OEC will be described here in order to help to understand the reactions of artificial molecular catalysts.
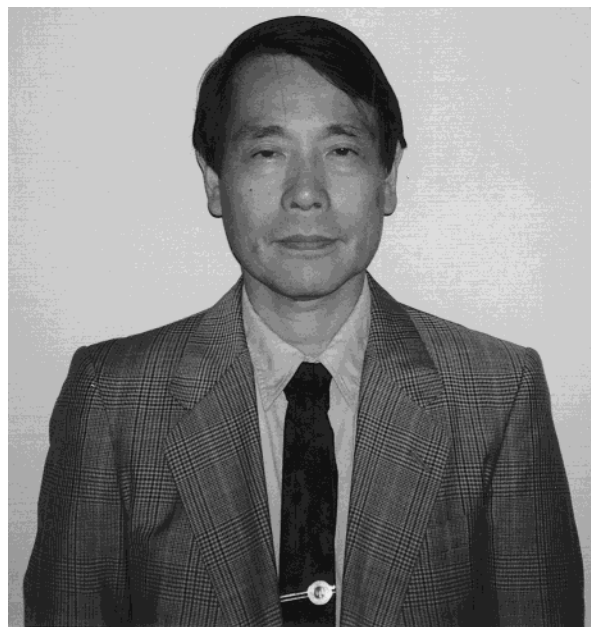
Electron paramagnetic resonance (EPR) spectrometry has revealed two characteristic EPR signals associated with the S_2 oxidation state: one is a
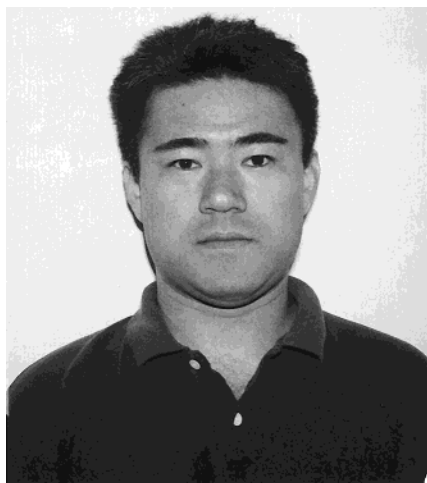
Masayuki Yagi was born in Japan in 1968. After receiving his B.Sc. degree in Chemistry from Ibaraki University in 1991, he did Ph.D. research on water oxidation chemistry and charge-transfer reactions in solid matrixes supervised by Professor Masao Kaneko; he received his Ph.D. degree from Saitama University in 1996. He joined the faculty of Niigata University (Japan) in 1996 and was promoted to Associate Professor of Chemistry in 1997. He has been the recipient of the Japan Society for the Promotion of Science Postdoctoral Fellowship for Research Abroad since 1999 and has worked on photosynthesis and its synthetic model of manganese complexes with Professor G. Charles Dismukes as a Visiting Fellow at Princeton University. His research interests include artificial photosynthesis, multi-electron-transfer reactions, and photo- and electrochemistry of functional metal complexes.

Masao Kaneko was born in Yokohama, Japan, and received his B.Sc. (1965). M.Sc. (1967), and Ph.D. (1970) degrees in Polymer Chemistry from Waseda University in Tokyo, Japan. After assistantship at the same University, he worked as a Visiting Researcher in the Institute of Organic Chemistry in the Free University of West Berlin with a DAAD fellowship (1971–1972) and Alexander-von-Humboldt fellowship (1972–1973). He became a Senior Researcher at the Nissan Petroleum Chemical Co., Ltd. (1973), Senior (1975) Researcher at the Institute of Physical and Chemical Research (RIKEN Institute), and Associate Director at the Chemical Dynamics Laboratory at the RIKEN Institute (1985). He moved to Ibaraki University in 1993, and he is now Full Professor in the Faculty of Science at Ibaraki University. His research interests are focused on constructing an artificial photosynthetic system for creating energy resources from solar energy and water.
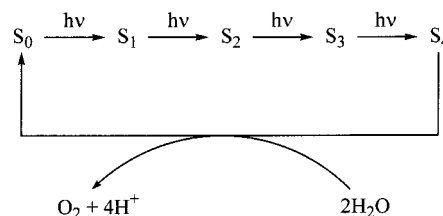
multiline EPR signal centered at $g = 2$ with a hyperfine structure characteristic of tetramanganese cluster, and the other is a broader signal at $g = 4.1$.[13,28,29] Although there are controversies on the interpretation of these EPR signals, this result suggests that all four manganese centers are appreciably coupled to create the multiline EPR signal. Dismukes et al. recently showed that the EPR data for S_2 is consistent with the presence of a distorted cubane or incomplete-cubane core type structure for the tetramanganese cluster in comparison with the EPR data of a model complex with Mn_4O_4 cubane core structure.[20] ^{55}Mn electron spin−echo-electron nuclear double resonance (ESE-ENDOR) study of the S_2 state concluded that a spin-coupled tetranuclear model for Mn cluster provides the best parameter set for simulation of both EPR and ^{55}Mn ENDOR spectra.[30] Although the precise structure of the Mn cluster remains an issue of intense interest, it is generally accepted that the manganese aggregate consists of four Mn atoms.

During each of the first two steps in the Kok cycle (S_0 to S_1 and S_1 to S_2 transitions), one oxidizing equivalent is stored on the manganese cluster, respectively. The S_1 and S_2 states are characterized by X-ray absorption near-edge spectroscopy (EXANES), and the most likely sets of manganese oxidation states are $2Mn^{III}-2Mn^{IV}$ for S_1 and $Mn^{III}-3Mn^{IV}$ for S_2.[16,23] For the S_2 to S_3 transition, opinion is however divided between accumulation of the third oxidizing equivalents on the manganese cluster[31] versus oxidation of a different moiety, either histidine[32] or bridging oxo, in the cluster.[16] For the final $S_3 \rightarrow [S_4] \rightarrow S_0$ step (transient S_4 state is unstable), the reduction of tyrosyl radical ($Y_Z^{\cdot}$) occurs with the production of O_2.[18,23]

Scheme 1.

$$S_0 \xrightarrow{h\nu} S_1 \xrightarrow{h\nu} S_2 \xrightarrow{h\nu} S_3 \xrightarrow{h\nu} S_4$$

$$O_2 + 4H^+ \qquad\qquad 2H_2O$$

Studies of the extended X-ray absorption fine structure (EXAFS) in the S_1 state revealed at least two 2.7 Å Mn···Mn vectors as well as a longer 3.3 Å Mn···Mn (or Mn···Ca) vectors, indicating that four Mn atoms are likely arranged in a tightly bridged low-symmetry Mn cluster.[16,23] Klein et al. proposed based on the EXAFS data a C-shape dimer-to-dimer core structure in which the Mn cluster is composed of two di-μ-oxo Mn dimer units linked by mono-μ-oxo and di-μ-carboxylate bridges.[16,23]

Chloride ion is an essential cofactor for O_2 evolution necessary to promote the S_2 to S_3 and S_3 to S_0 transitions but not essential for the S_0 to S_1 and S_1 to S_2 ones. The S_2 state formed in the absence of Cl^- does not exhibit either of the unusual S_2 EPR signals, but dark addition of Cl^- to such sample causes the multiline signal to form. Although Cl^- binding to the manganese complex has not yet been demonstrated by spectroscopic measurements, it is reasonable to conclude that Cl^- is a ligand to manganese in the higher S states.[23] Calcium is also required for O_2
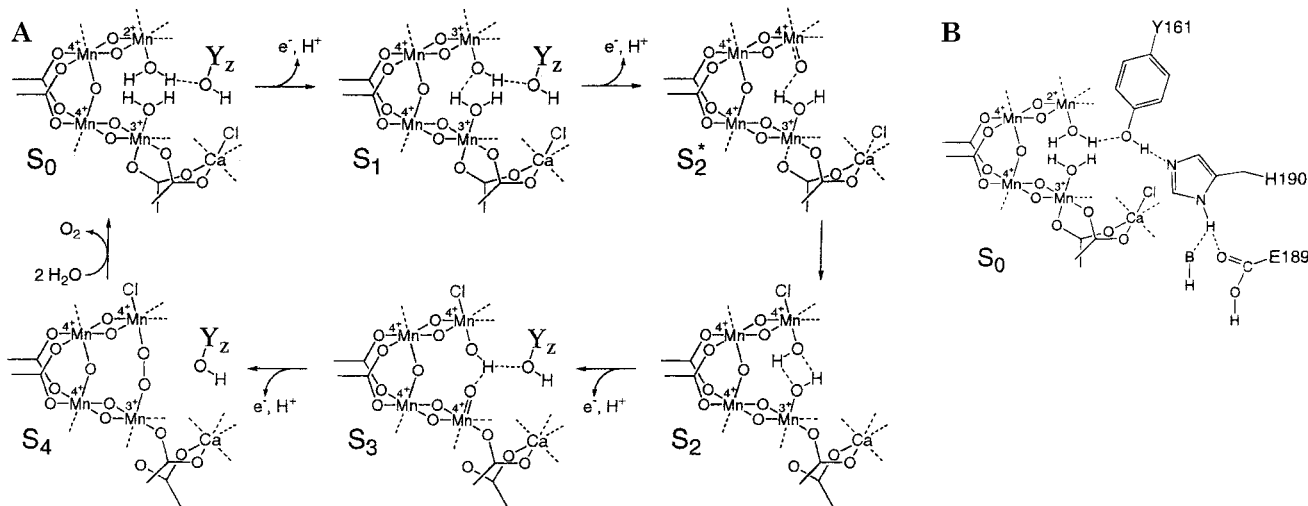
Figure 1. Proposed model of S state cycle (A) and structure of the S_0 state (B). (Reprinted with permission from ref 25. Copyright 1998 American Chemical Society.)

evolution.[23] Depletion of Ca^{2+} causes the Kok cycle to stop at an S_2 similar to Cl^- depletion. The available data show that calcium or (strontium) is essential to water oxidation. The calcium has been proposed to play a "gatekeeper" role controlling substrate (water) accessibility to the tetramanganese core during S-state transitions[34] and function to lower the activation barrier to formation of the anionic peroxo intermediate in the $S_3 \rightarrow S_0$ transition.[20] However, the functions of Cl^- and Ca^{2+} in the OEC activity are not yet sufficiently clear.

As hypotheses for the water oxidation mechanism at the OEC, structural conversion between a Mn_4O_4 cubane and Mn_4O_6 adamantane-type cores proposed by Brudvig and Crabtree[21] as well as the conversion between a Mn_4O_2 butterfly and Mn_4O_4 cubane-type cores proposed by Vincent and Christou[22] have been made more than a decade ago. On the basis of EXAFS and Mn K-edge spectroscopy data, Yachandra and Klein proposed another possible mechanism in which one di-μ-oxo-dimer with Mn(III,III) in a C-shape dimer-to-dimer tetramanganese is proposed to be redox active, and Mn(IV,IV) dimer is redox inert in the whole catalytic cycle.[16] In the transition of S_2 to S_3, the Mn center is not oxidized but the μ-oxo bridge is oxidized to oxyl radical. This idea comes from the increase of one Mn–Mn distance from 2.7 to 2.9 Å observed in EXAFS data. The elongation of the Mn–Mn distance is explained by the delocalization of an oxidative equivalent over the entire Mn_2O_2 unit. The di-μ-oxyl radical is proposed to be formed by a further oxidation in the S_4 state. This di-μ-oxyl radical spontaneously produces O_2 molecule and an S_0 state possibly via the μ-η^2:η^2-peroxo intermediate species. On release of O_2, two hydroxyl groups are incorporated into the Mn cluster from two water substrates with the concomitant release of two protons. However, there is no direct spectroscopic evidence for formation of a μ-oxyl radical bridge.

Recently Babcock et al. proposed a new model (Figure 1A) where tyrosyl radical ($Y_Z^\bullet$) acts as a hydrogen-atom abstracter rather than as a simple electron-transfer cofactor and releases a proton to His190 on oxidation of Y_ZH by P_{680}, after which this proton is ultimately delivered to bulk aqueous phase.[19,23–25] The C-shape dimer-to-dimer tetramanganese (Mn^{II}, Mn^{III}, $2Mn^{IV}$) core with two substrate water molecules as terminal ligands was employed in the S_0 state (Figure 1B). The reaction of protons and electrons is postulated to be coupled on each S-state advancement step. On S_3 to S_4 transition, hydrogen-atom transfer produces a manganese-bonded oxyl radical that attaches to a terminal oxo (Mn=O) of another manganese ion in concert with the hydrogen-atom transfer to produce a peroxide species bound to manganese. To complete the S-state cycle, the manganese peroxo bond cleaves, releasing O_2 and allowing water to bind to newly vacated coordination sites. The model (Figure 1A) proposed by Babcock et al. is different from previous models in that it employs minimal structural changes of the manganese cluster and is thermodynamically just based on bond enthalpy consideration.[33] However, it would be difficult to know which structural changes actually occur before structural information on the S states is obtained. The model of Babcock et al. also invokes large-scale movement of Cl^- in the process and has no clear essential function for calcium other than a holding site for Cl^-. Irrespective of these circumstances, the hydrogen-atom transfer mechanism is an appealing idea based on the reasonable thermodynamic difference of the bond enthalpies.

In another model proposed by Pecoraro, two di-μ-oxo Mn dimers function independently, one to oxidize water to peroxide and the other to oxidize peroxide to O_2.[35] $Mn^V=O$ species is proposed to be generated in the S_4 state and attacked by a strongly nucleophilic hydroxyl group bound to Ca (or alternatively Mn) to form a peroxide intermediate. The transiently formed peroxide intermediate is two-electron-oxidized by another di-μ-oxo Mn dimer in the C-shape dimer-to-dimer to produce O_2 and the S_0 state. In this model, water oxidation is separated into two two-electron steps via hydroxide formation so that it does not need to overcome the energetic barrier of the four-electron process in one step. A similar mechanism was proposed involving $Mn^V=O$ intermediate species in the S_4 state.[26] It is hypothesized in this mechanism that

O−O bond formation is achieved by nucleophilic attack on the $Mn^V=O$ by a hydroxide ligated to calcium ion, and ultimately the S_4 state is converted to S_0 with a concomitant release of O_2. The functional role of chloride is proposed to be a bridge that communicates the formation of the $Mn^V=O$ to a calcium-bound hydroxide so that a nucleophilic hydroxide would be created in concert with an electrophilic $Mn^V=O$ to facilitate formation of the O−O bond. These mechanisms involving the $Mn^V=O$ species are only based on $Ru^V=O$ chemistry[36] and the formation of the $Mn^V=O$ intermediate[37] evidenced in epoxidation catalyses by $[Mn^{III}(salen)]^+$ (salen = N,N'-bis(salicylidene)ethylenediamine dianion), and the evidence of $Mn^V=O$ intermediate formation in water oxidation is not basically obtained yet.

Siegbahn and Crabtree proposed a mechanism involving only one redox-active manganese atom of the Mn_4 cluster on the basis of quantum chemical calculation of a simple model complex.[27] In this proposal, the C-shape core structure was also adopted. An unreactive Mn(IV)=O oxo is formed as a terminal ligand in the S_2 state followed by its conversion to a reactive Mn(IV)−O• oxyl formed at the S_3 level. This oxyl radical couples with an outer-sphere water molecule to produce the O−O bond formation. A Mn−O−O−H species in the S_3 state is proposed to lose a hydrogen atom to give O_2. They further proposed a role for the Ca^{2+} cofactor in this mechanism to bring about a change from five- to six-coordination in the S_2 state, necessary for the formation of a reactive oxo in the S_3 state.[27] Siegbahn et al. reinvestigated and elaborated on their own mechanism by an advanced calculation of a trimanganese oxo (not tetramanganese) model system.[38] It is confessed that oxygen radical is very difficult to be formed on a terminal oxo but rather should be on a μ-oxo bridge between Mn ions. The O−O bond is suggested to be formed from external water (providing the second oxygen in O_2) taken in an incomplete cubane core with a missing corner ($Mn_2CaO(OH)(OH_2)_2$; $Mn^{IV}-Mn^{IV}$ in the S_3 state) comprised of one of the two di-μ-oxo Mn dimer parts and an aqua calcium ion.

A three-dimensional structure of plant photosystem II subcomplex, containing the proteins D1, D2, CP47, and cytochrome b-559 but lacking the OEC, was determined by electron crystallography at 8 Å resolution.[39] Very recently, crystallized PS II capable of O_2 evolution and H^+ release was isolated.[40] The crystal structure at 3.5 Å resolution has been communicated at several conferences, although the analysis results are still insufficient.[41] Resolution of the debate over the structure of the OEC will be achieved by determination of the complete crystal structure of PS II with an intact OEC, which might help to investigate the photosynthetic water oxidation and the role of cofactors in the OEC.

III. Water Oxidation by Molecular Catalysts in Homogeneous Systems

Homogeneous systems are convenient to understand the basic catalytic aspect of molecular catalysts. A few Mn and Ru complexes have been reported which can evolve O_2 from water in homogeneous
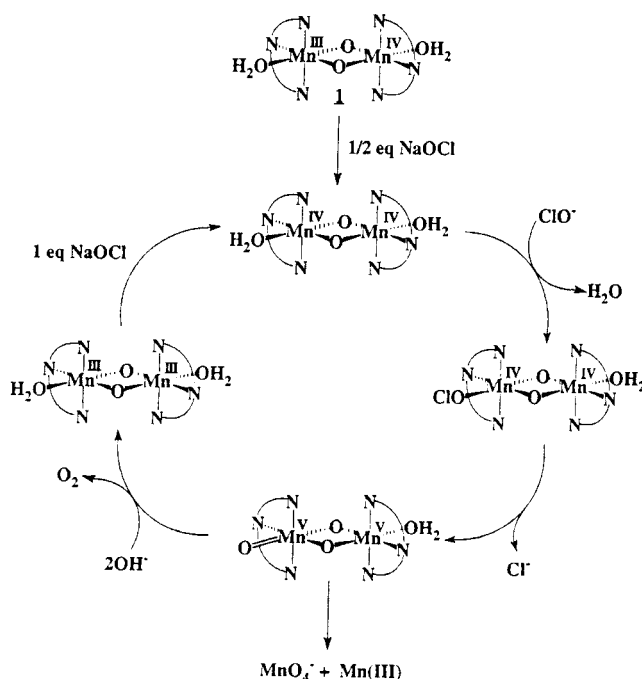

Figure 2. Proposed reaction mechanism for O_2 formation from the reaction of [(terpy)(H_2O)Mn(μ-O)$_2$Mn(terpy)-(H_2O)]$^{3+}$ with NaClO. (Reprinted with permission from ref 45. Copyright 1999 American Association for the Advancement of Science.)

system. Mn complexes have been studied in relation to the structure and function of the OEC.[6−9] Although many useful Mn complexes have given guided thoughts on the structure of the OEC, most of these have not been capable of oxidizing water to O_2. Only one example of water oxidation by Mn complexes, which is known to be a structural model of OEC, was reported in 1986, in which [(bpy)$_2$Mn^{III}(μ-O)$_2$Mn^{IV}-(bpy)$_2$]$^{3+}$ (bpy = 2,2′-bipyridine) works as a heterogeneous catalyst to evolve O_2 in its aqueous suspension (The amount of complex is beyond its solubility in water).[42] Covalently linked manganese porphyrin dimers were reported to oxidize water in a homogeneous solution, although it is far from the structural model of OEC.[43] Herein we review recent progress in water oxidation by molecular catalysts in homogeneous systems

Limburg and Brudvig reported that O_2 is evolved by the reaction of [Mn(dpa)$_2$]$^-$ (dpa = dipicolinate) with a highly oxidizing oxygen-atom transfer reagent, potassium peroxymonosulfate in an acetate buffer aqueous solution. This reaction produced a Mn$_2$(III/IV) dimer as an intermediate, proposed to be involved in O_2 evolution, competing with the thermodynamically favored formation of MnO$_4^-$, which is unreactive as a catalyst for O_2 evolution.[44] They concluded that di-μ-oxo Mn$_2$(III/IV) binuclear complexes with planar tridentate ligands are sufficient for O_2 evolution by producing an open coordination site for water. However, the source of oxygen atoms for O_2 remains controversial. It could originate entirely from the peroxymonosulfate oxidant rather than water (in contrast to their claim for water oxidation.) On the basis of this result, [(terpy)(H_2O)Mn(μ-O)$_2$Mn(terpy)-(H_2O)]$^{3+}$ (terpy = 2,2′:6′,2″-terpyridine) was synthesized and structurally characterized by their group[45]
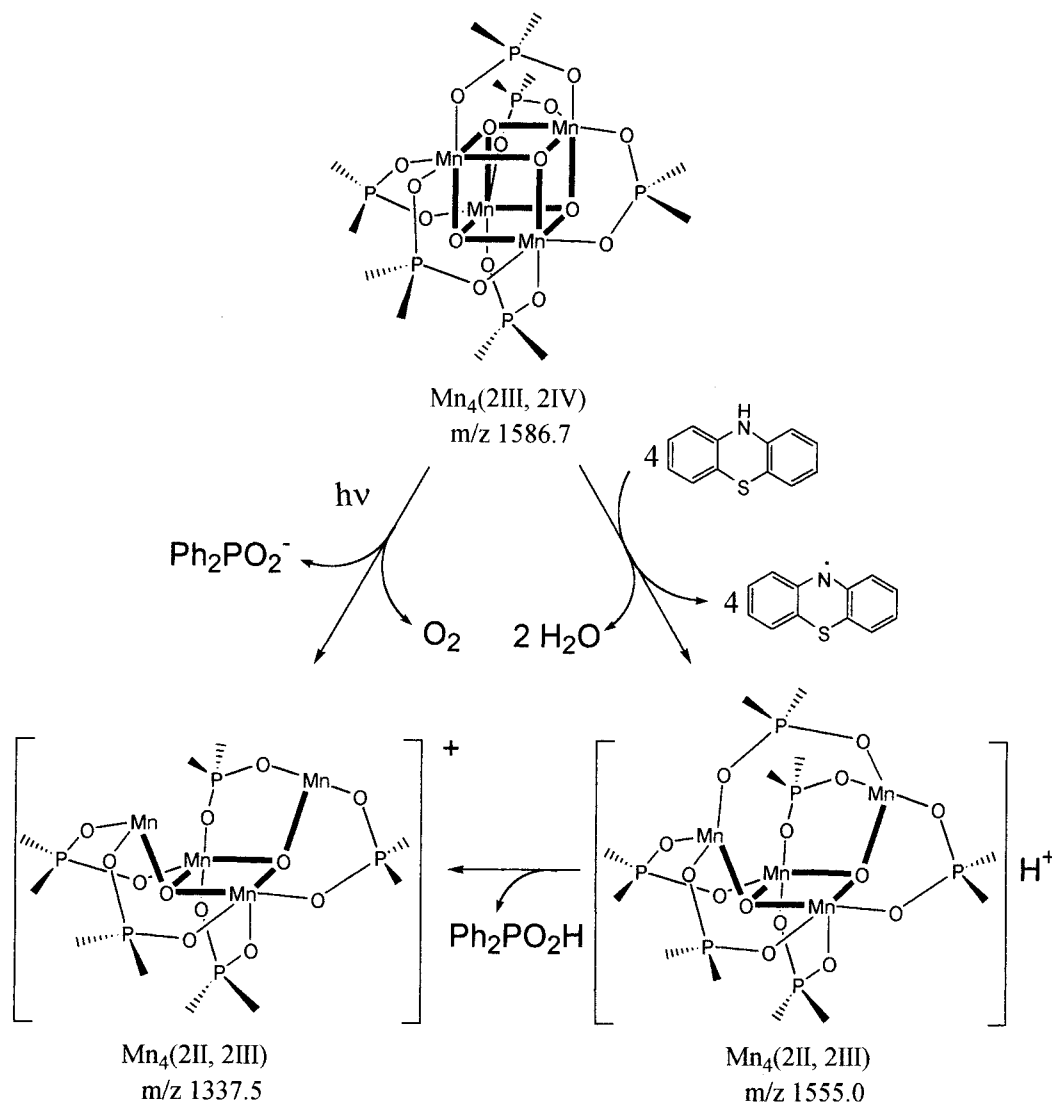
Figure 3. Reactions of the manganese−oxo cubane, $L_6Mn_4O_4$, L = diphenylphosphinate; $Ph_2PO_2^-$, in the gas phase (left) and as a solute in acetonitrile/methylene chloride solvent (right). (Reprinted with permission from ref 52. Copyright 2000 American Chemical Society.)

and Collomb et al.[46] Subsequently, Limburg and Brudvig demonstrated O_2 evolution by the reaction between the complex and sodium hypochlorite (NaClO), which is also a highly oxidizing oxygen-atom transfer reagent.[45] The complex was decomposed to MnO_4^- during the catalytic cycle, leading to the end of the cycle after about 6 h with a maximum turnover of the catalyst of 4. They showed by an [18]O isotope-labeling experiment that the O atom comes from water not the oxidant. However, they are completely missing isotope exchange between ClO^- and $H_2(^{18}O)$ in the [18]O isotope-labeling O_2 evolution experiment. Their results on isotope experiments cannot be accepted without the isotope exchange data in a solution. (Subsequently ClO^- was identified as the source of O_2 and not water.[47]) They proposed the catalytic cycle for O_2 evolution in Figure 2, which involves a hypothesized intermediate of di-μ-oxo $Mn_2^{V/V}$ dimer with terminal manganyl (Mn=O). This intermediate has not been detected yet but is proposed to react with OH^- to produce O_2 and di-μ-oxo-diaquo-$Mn_2^{III/III}$ dimer. If experimental evidence could be found for such a manganyl intermediate, it might support the

Mn=O formation proposed as an intermediate in the OEC. However, the mechanism of O_2 formation in this system is almost completely unclear. It could involve reaction of terminal Mn=O or μ-oxo with OH^- or even disproportionation of $2ClO^- \rightarrow O_2 + 2Cl^-$, which is known to be catalyzed by Mn(II) and other Lewis acids.[48]

Ruettinger and Dismukes reported the synthesis and characterization of a tetramanganese complex $[L_6Mn_4O_4]$ (L = diphenylphosphinate) with a Mn_4O_4 ($2Mn^{III}, 2Mn^{IV}$) cubane core (Figure 3)[49] and succeeded in isolation of the one-electron-oxidized $[L_6Mn_4O_4]^+$ ($Mn^{III}, 3Mn^{IV}$) cubane complex.[50] The redox potential of $[L_6Mn_4O_4]/[L_6Mn_4O_4]^+$ is 1.38 V vs NHE, which is considerably greater than those found for the dimanganese (III,IV)/(III,III) couple and the majority of known (IV,IV)/(III,IV) couples.[49] The $[L_6Mn_4O_4]$ cubane complex reacted with the hydrogen-atom donor, phenothiazine in a CH_2Cl_2 solution, forming $[L_6-Mn_4O_2]$ and $[L_5Mn_4O_2]^+$ as well as releasing two water molecules from the core.[51] This result shows that two of the corner oxos of the cubane can be converted into two labile water molecules. $[L_6Mn_4O_2]$

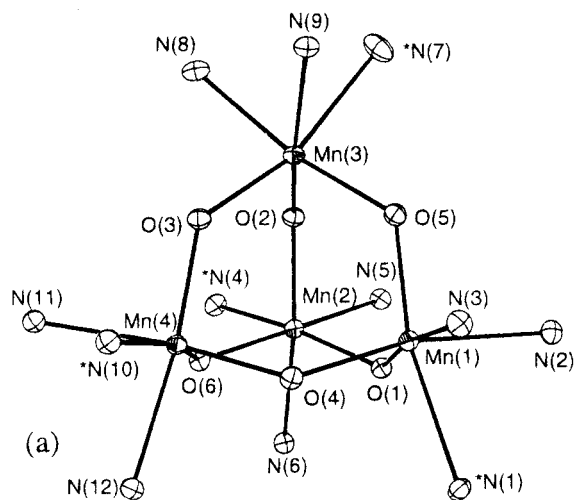**Figure 4.** Structure of the adamantane-like complex $[Mn^{IV}_4O_6(bpea)_4](ClO_4)_4$ (Reprinted with permission from ref 53. Copyright 1998 American Chemical Society.)

and $[L_5Mn_4O_2]^+$ were found to contain the Mn_4O_2 core, and structural data were reported. These were hypothesized to represent "incomplete cubane" and "butterfly" complexes. It was found that UV light absorption by $[L_6Mn_4O_4]$ converts two of the corner oxos of the cubane into an O_2 molecule, which is released only if one of the bridging chelates is also released to form $[L_5Mn_4O_2]^+$.[52] The evolution of O_2 molecule from Mn_4O_4 cubane core was corroborated by the detection of $^{18}O_2$ from $[L_6Mn_4(^{18}O)_4]$. It was suggested that intramolecular O–O bond coupling of the oxo bridges for production of O_2 is possible in complexes containing the longer $Mn-O(\mu_3\text{-oxo})$ bonds of the cubane core (1.95 Å) than that observed for $[Mn_2O_2]^{3+}$ cores (1.8 Å). The $[Mn_4O_4]^{n+}$ cubane core is a reactive intermediate for the chemical transformation of the oxo bridges to both water and O_2 (Figure 3), which showed that the cubane–butterfly rearrangement hypothesis for the OEC cannot be excluded merely on the basis of the limited structural data available at the present time.

A Mn_4O_6 adamantane-like core was formed in complexes $[Mn^{IV}_4O_6(bpea)_4](ClO_4)_4$ and $[Mn^{III}Mn^{IV}_3O_6\text{-}(bpea)_4](ClO_4)_3$ (dpea = N,N-bis(2-pyridylmethyl)-ethylamine) (Figure 4). These complexes exhibited two proton-coupled electron-transfer ($e^-/2H^+$) steps between $[Mn^{IV}_4O_6(bpea)_4]^{4+}$ and $[Mn^{III}Mn^{IV}_3O_4(OH)_2\text{-}(bpea)_4]^{5+}$ in the pH range 3.51–1.05 and are considerably stronger oxidants than the earlier triaza-cyclononane derivatives.[53] However, neither water oxidation nor any other oxidation process was investigated in this work.

The electrochemistry of $[Mn^{III}(bpy)_3]^{3+}$ and $[(bpy)_2Mn^{III}(\mu\text{-}O)_2Mn^{IV}(bpy)_2]^{4+}$ in aqueous bpy/bpyH$^+$ buffer and acetonitrile solutions was investigated, and a new and easy synthesis of a linear tetranuclear Mn complex $[Mn^{IV}_4O_6(bpy)_6]^{4+}$ is shown.[54] It is suggested that $[(bpy)_2Mn^{III}(\mu\text{-}O)_2Mn^{IV}(bpy)_2]^{4+}$ cannot act as a homogeneous electrocatalyst for water oxidation in an aqueous media since its one-electron-oxidized $Mn^{IV}-Mn^{IV}$ species is unstable to lead the stable linear tetranuclear species $[Mn^{IV}_4O_6(bpy)_6]^{4+}$ in an aqueous bpy/bpyH$^+$ buffer, indicating that the $[Mn^{IV}_4O_6(bpy)_6]^{4+}$ complex cannot be involved in O_2

evolution.[54] Elsewhere, Mn_4-Ca_2 aggregates have been synthesized and their catalase activity reported (dehydrogenation of H_2O_2 to O_2), but water oxidation was not reported.[55]

$[(bpy)_2(H_2O)Ru^{III}(\mu\text{-}O)Ru^{III}(H_2O)(bpy)_2]^{4+}$ and its derivatives are known to be water oxidation catalysts, and many works have been reported on the redox and structural chemistry of the complex for understanding the mechanism of water oxidation.[56] However, the catalytically active forms and the mechanism have remained unsolved. Chronister and Meyer et al. reported, using global kinetic analysis of UV–vis absorption data, that water oxidation by the complex is a complex process featuring stepwise redox and cross reactions among five different oxidation states of the dimer when using of 2–5 equiv of Ce(IV) as oxidant.[57] They concluded that the rate-determining step is not water oxidation but rather changes with time, from oxidation of Ru^{III}ORu^{IV} by comproportionation with Ru^{IV}ORu^V to oxidation of Ru^{IV}ORu^V by Ce-(IV) as the reaction proceeds to completion.

The nonisolated complex $[(terpy)(H_2O)_2Ru^{III}(\mu\text{-}O)\text{-}Ru^{III}(H_2O)_2(terpy)]^{4+}$ was formed in solution from an isolated $[(terpy)(C_2O_4)_2Ru^{III}-O-Ru^{III}(C_2O_4)_2(terpy)]^{4+}$ complex by a ligand-exchange reaction.[58] The solution chemistry and water oxidation of this complex were reported. However, the turnover number (mol of O_2 evolved/mol of complex) does not exceed unity, indicating that this complex is not a catalyst. Oxidative cleavage of the complex to Ru^{VI}(terpy)(O)$_2$(OH$_2$)]$^{2+}$ in competition with O_2 evolution was considered to be one of the reasons why the complex does not work as a catalyst.[58]

Water oxidation catalysis by ammine-coordinated Ru complexes was investigated in a homogeneous aqueous solution to evaluate the influence of structure on their catalytic activity and mechanism.[59–65] An aqueous solution of $[(NH_3)_5Ru^{III}(\mu\text{-}O)Ru^{IV}(NH_3)_4\text{-}(\mu\text{-}O)Ru^{III}(NH_3)_5]^{6+}$ (Ru-red) with a large excess of a Ce(IV) oxidant induced visible bubble formation due to O_2. The first-order dependency of O_2 evolution rate on the catalyst concentration (at low catalyst concentration range) showed that water oxidation is catalyzed by one molecule of Ru-red, which works as a four-electron oxidation catalyst.[59] The initial turnover rate of Ru-red in the catalysis was 5.1×10^{-2} s^{-1}, and the total turnover number was 75 in 3 h. Ru-red underwent bimolecular decomposition to deactivate in highly concentrated conditions, producing N_2 by oxidation of the ammine ligands, competitive with the catalytic O_2 evolution.[59] Such decomposition is an essential problem for oxidation catalysts by metal complexes with organic ligands. Incorporation of Ru-red into heterogeneous matrixes, such as a polymer membrane, remarkably suppressed the bimolecular decomposition, thereby increasing the apparent catalytic activity, as mentioned later in section IV. Dinuclear complexes of $[(NH_3)_5Ru^{III}(\mu\text{-}O)Ru^{III}\text{-}(NH_3)_5]^{4+}$[60] and $[(NH_3)_3Ru^{III}(\mu\text{-}Cl)_3Ru^{II}(NH_3)_3]^{2+}$[61] showed catalytic behavior similar to Ru-red, e.g., both complexes acted as four-electron oxidation catalysts but underwent bimolecular decomposition under high catalyst concentrations. The initial turnover rate of the $[(NH_3)_3Ru(\mu\text{-}Cl)_3Ru(NH_3)_3]^{2+}$ for the catalysis was

Table 1. Comparison of Catalytic Activity (kO_2) of Various Ruthenium Complexes for Water Oxidation

| | $kO_2/10^{-3}$ s^{-1} ^{a} | | | |
| | homogeneous system^b | hetetogeneous system^c | catalytic activity | ref |
system				
$[(NH_3)_5Ru^{III}(\mu\text{-}O)Ru^{IV}(NH_3)_4(\mu\text{-}O)Ru^{III}(NH_3)_5]^{6+}$ (Ru-red)	51	45	four-electron oxidation	59
$[(bpy)_2(H_2O)Ru^{III}(\mu\text{-}O)Ru^{III}(H_2O)(bpy)_2]^{4+}$	4	2.4	four-electron oxidation	76
$[(NH_3)_5Ru^{III}(\mu\text{-}O)Ru^{III}(NH_3)_5]^{4+}$	13	13	four-electron oxidation	60
$[(NH_3)_3Ru^{III}(\mu\text{-}Cl)_3Ru^{II}(NH_3)_3]^{2+}$	56	63	four-electron oxidation	61
$[Ru^{III}(NH_3)_6]^{3+}$	0.014 ^{d}	0.035^e	two-electron oxidation	62
$[Ru^{III}(NH_3)_5Cl]^{2+}$	0.31 ^{d}	2.7^e	two-electron oxidation	63
cis-$[Ru^{III}(NH_3)_4Cl_2]^+$	2	14	four-electron oxidation	65
$[Ru^{III}$ (en)$_3]^{3+}$	0.17 ^{d}	0.085^e	two-electron oxidation	64
IrO$_2$		1.4^f		76
RuO$_2$		0.75^f		76
Pt-black		0.25^f		76

^{a} Turnover rate calculated from kinetic analysis based on first-order O$_2$ evolution and second-order deactivation. ^{b} Aqueous solution. ^{c} Nafion membrane. ^{d} Maximum turnover rate at a low concentration in an aqueous solution. ^{e} Intrinsic catalytic activity obtained by an activity analysis based on the molecular distribution (see section IV). ^{f} Suspension system.

5.6×10^{-2} s^{-1}, which is the most active molecular catalyst studied to date.[61]

Mononuclear Ru(III) complexes of $[Ru^{III}(NH_3)_6]^{3+}$ [62] and $[Ru^{III}(NH_3)_5Cl]^{2+}$ [63] also work as water oxidation catalysts. However, the O$_2$ evolution rate was found to be second order with respect to the catalyst concentration, in contrast to first order for the multinuclear complexes. This result showed that two molecules of the complex catalyzed water oxidation cooperatively (so-called cooperative catalysis), indicating a two-electron oxidation per catalyst molecule. These complexes also underwent bimolecular decomposition under high catalyst concentration conditions in an aqueous solution. Catalysis by $[Ru^{III}(en)_3]^{3+}$ (en = ethylenediamine) was compared to $[Ru(NH_3)_6]^{3+}$ in the hope that ammine chelate ligand might suppress or prohibit the decomposition which occurs by ligand oxidation.[64] However, the en chelate did not stabilize the catalyst against the decomposition.

cis-$[Ru^{III}(NH_3)_4Cl_2]^+$ [65] exhibited unique behavior compared to the other mononuclear Ru(III) complexes. The O$_2$ evolution rate was found to be first order with respect to the catalyst concentration. This first-order dependence means that the rate-limiting step in O$_2$ evolution requires only one molecule of cis-$[Ru(NH_3)_4Cl_2]^+$. This might be explained by several ways. One possibility involves a new mechanism by oxidation of two chloro ligands to hypochlorite to form cis-$[Ru(NH_3)_4(ClO)_2]^+$ as an intermediate in the catalysis. Ru(III) could then serve as a Lewis-acids catalyst to allow the hypochlorite ligands to disproportionate by intramolecular coupling to produce O$_2$.[65] However, no direct spectroscopic evidence for the oxidation of the chloro ligands to hypochlorite was obtained.

The catalytic activities of Ru complexes are summarized in Table 1. Comparison between multinuclear and mononuclear complexes shows that the former complexes are more active catalysts than the latter complexes. This is probably because the multinuclear structures are capable of forming oxidized intermediates with four delocalized oxidizing equivalents compared with only two oxidizing equivalents in the mononuclear complexes. Multinuclear structures are important for developing efficient molecular catalysts.
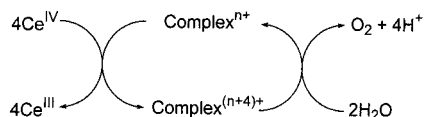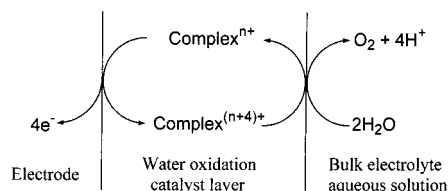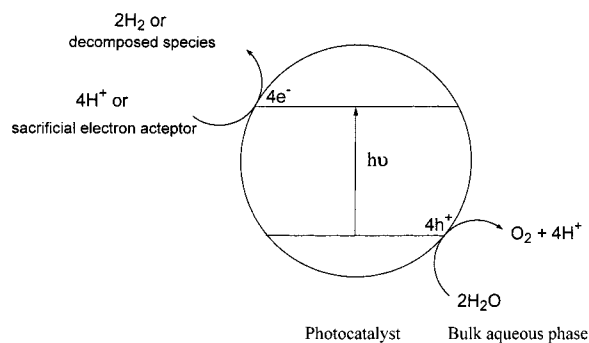
As for the mononuclear complexes, the order of the catalytic activity was cis-$[Ru(NH_3)_4Cl_2]^+ \gg [Ru(NH_3)_5Cl]^{2+} \gg [Ru(NH_3)_6]^{3+}$, showing that the activity of the complex increases remarkably on substitution of the ammine ligand by chloro ligand. Although the high catalytic activity of cis-$[Ru(NH_3)_4Cl_2]^+$ might be explained by its four-electron oxidation ability,[65] the comparison between $[Ru(NH_3)_6]^{3+}$ and $[Ru(NH_3)_5Cl]^{2+}$, both of which work as only two-electron oxidation catalysts (vide supra), requires other interpretations and remains a problem for future resolution. The above results shed light on the design of OEC models capable of evolving O$_2$ from water.

IV. Water Oxidation Catalysis and Activity Analysis in Heterogeneous Systems

Heterogeneous systems for water oxidation should be developed to design an artificial photosynthesis which is composed of a water oxidation catalyst, photoexcitation center, and carbon dioxide or proton reduction catalyst.[2,4] The aspect and activity of a molecular catalyst for water oxidation should be necessary to be comprehended in a heterogeneous matrix. However, very few works have been reported on water oxidation in heterogeneous systems confining molecular catalysts.

It is important to study factors affecting the activity and stability of the catalysts and to establish activity models involving these factors in order to optimize water oxidation catalysis. However, there had been no report on such an analysis model for water oxidation catalysis in a heterogeneous system before the recent work on the ammine-coordinate Ru complexes confined in heterogeneous systems such as a polymer membrane,[59-70] inorganic particle,[71-74] and intercalation compound.[75]

Three different approaches are figured out to demonstrate water oxidation in a heterogeneous system. One is a chemical method (Scheme 2) using strong oxidants such as Ce^{4+}, $[Ru(bpy)_3]^{3+}$, and MnO$_4^-$, and this method is easily applicable to both homogeneous and heterogeneous systems to compare both catalyses. Second is an electrochemical method by potentio-controlled electrolysis. This method is available in a solution containing a molecular cata-

Scheme 2. Chemical Water Oxidation Catalysis

Scheme 3. Electrochemical Water Oxidation Catalysis

Scheme 4. Water Oxidation by Photocatalysts

Nafion

Figure 5. Chemical structure of Nafion.

Figure 6. Relationships between the apparent catalytic activity, k_{app} (s^{-1}), and complex concentration in the (a) aqueous solution and (b) Nafion membrane for a Ru-red system. The solid line shows a calculation curve based on eq 3 when $k = 4.4 \times 10^{-2}$ s^{-1} and $r_d = 1.23$ nm. (Reprinted with permission from ref 59. Copyright 1996 American Chemical Society.)

lyst but has a disadvantage in evaluation of its catalytic activity (turnover rate; turnover number/ unit time). The catalyst cannot work away from an electrode surface in a bulk solution and must diffuse to an electrode surface to work as a catalyst. Therefore, the catalytic activity includes the contribution of diffusion and depends on a scale of the reaction system. Catalyst-modified electrodes are utilized for electrocatalysis (Scheme 3) in which molecular catalysts are attached to an electrode surface by using heterogeneous matrixes such as polymer membranes, ion-exchange resins, and intercalation compounds or directly by chemical and physical interaction between the molecules and surface. Irrespective of solution and heterogeneous matrix systems, the charge transfer from the electrode to the catalysts is an important factor in evaluating the catalytic activity. Third is photochemical water oxidation by photocatalysts (Scheme 4). In this method, the holes generated by photoexcitation on n-type semiconductors oxidize water to O_2. The electrons generated by photoexcitation react with the electron acceptor (sacrificial acceptor in many cases). If a proton in the bulk solution works efficiently as an electron acceptor, this corresponds to a complete water splitting to O_2 and H_2. However, a complete water splitting is limited to photocatalysis by UV light excitation to date (no example for this reaction by visible light).

Herein we review aspects of molecular catalysts and analyses of the activity and stability of the catalysts in heterogeneous systems. In section IV.A, a chemical water oxidation system using Ce(IV) oxidant is described, followed by an electrochemical water oxidation system in section IV.B. The reaction of the molecular catalysts confined in the polymer
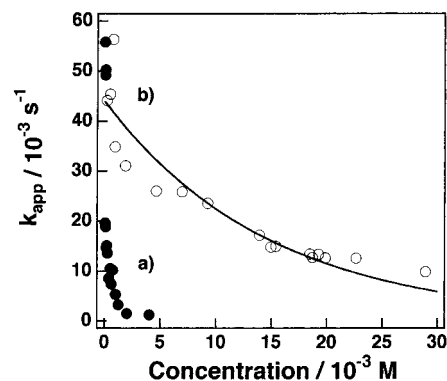
membrane is focused on in both sections. In section IV.C, photocatalysts capable of splitting water to O_2 and H_2 by UV irradiation as well as interesting progress on photocatalysts are picked up to discuss the heterogeneous water oxidation catalysis.

A. Chemical Water Oxidation

In a Nafion membrane (Figure 5), water oxidation catalysis by ammine-coordinated Ru complexes have been demonstrated using a Ce(IV) oxidant.[59-65,76] The complexes can work as active water oxidation catalysts in the membrane as well as in a solution. Importantly, bimolecular decomposition (see section III) of the catalyst was remarkably suppressed by incorporating it into the membrane[59-65] leading to high activities at high concentrations, as shown in Figure 6. From kinetic analysis based on competitive reactions of water oxidation and bimolecular decomposition of the catalyst, the first-order rate constant of O_2 evolution (4.5×10^{-2} s^{-1}) in the membrane was shown to be close to that (5.1×10^{-2} s^{-1}) in an aqueous solution of Ru-red,[59,77] indicating no significant loss of its intrinsic activity. On the contrary, the second-order rate constant for deactivation by bimolecular decomposition decreased by 2 orders of magnitude by incorporating the catalyst into the membrane (5.2×10^2 dm^3 mol^{-1} s^{-1} in the homogeneous solution, 5.6 dm^3 mol^{-1} s^{-1} in the membrane).[59] This was explained by suppression of physical diffusion
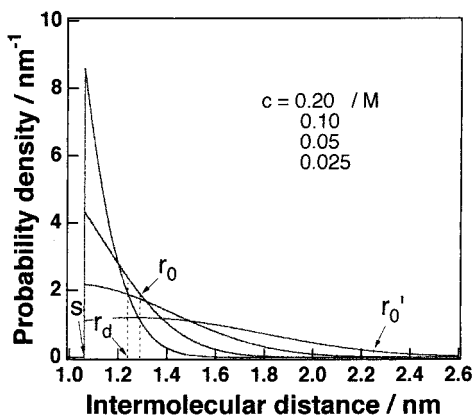
Figure 7. Intermolecular distance distribution between the nearest-neighbor molecules in the membrane for various concentrations. s is the contact distance of the catalyst, r_d is the critical decomposition distance, and r_0 and r_0' are charge-transfer distances in the absence and the presence of p-Cre, respectively. The values $s = 1.06$ nm and $\alpha = 5.1$ are used for the calculation. (Reprinted with permission from ref 67. Copyright 1997 American Chemical Society.)

of the catalyst in the membrane, which prohibits a bimolecular decomposition by collision of the catalysts.

Analysis of the catalytic activity was reported on the basis of the idea that the intermolecular distance between the catalysts is important for their activity (depending on the intermolecular interaction between the catalysts, e.g., bimolecular decomposition) in a system where molecular catalysts are immobilized in a polymer matrix. For the activity analysis, the intermolecular distance distribution was taken into account rather than the average intermolecular distance assuming a random dispersion of the catalyst. The intermolecular distance distribution between the nearest-neighbor molecules given by eq 2[59,63,66,67] was applied (Figure 7).

$$P(r) = 4\pi r^2 N_A \alpha c \times$$
$$10^{-24} \exp[-4\pi(r^3 - s^3)N_A \alpha c \times 10^{-24}/3] \quad (2)$$

In eq 2, $P(r)$ (nm^{-1}), N_A (mol^{-1}), α, c (mol dm^{-3}), and s (nm) are the probability density that the center-to-center distance between the nearest-neighbor molecules is r (nm), Avogadro's number, the degree of the localization of the catalyst in the membrane,[78] catalyst concentration in a membrane, and the contact distance between the catalysts,[79] respectively.

When a critical decomposition distance, r_d (nm), was assumed as the distance within which catalysts undergo a bimolecular decomposition, the apparent catalytic activity, k_{app} (s^{-1}), is given by eq 3.[59]

$$k_{app} = k \exp(-4\pi(r_d^3 - s^3)\alpha c N_A \times 10^{-24}/3) \quad (3)$$

where k is a constant to represent the intrinsic activity of the catalyst without bimolecular decomposition. The best fit of eq 3 to the experimental data (Figure 6b) gave $k = 4.4 \times 10^{-2}$ s^{-1} and $r_d = 1.23$ nm in a Ru-red/Nafion system.[59,80] This result shows that it is important to isolate the Ru-red catalyst by separating the intermolecular distance over 1.23 nm for optimizing the catalytic activity in the membrane.

This sheds light on the hitherto reported difficulty in developing active molecular catalyst for water oxidation in comparison with the OEC in photosynthesis where the Mn cluster center is isolated and stabilized against degradative oxidation of the surrounding ligands.

In the case of mononuclear Ru(III) complexes such as [Ru(NH$_3$)$_6$]$^{3+}$ [62] and [Ru(NH$_3$)$_5$Cl]$^{2+}$,[63] an optimum catalyst concentration in the membrane was exhibited, which was ascribed to both the cooperative catalysis and bimolecular decomposition. The turnover rates of both complexes also increased remarkably by incorporating them in a Nafion membrane, which was explained both by a favorable interaction of the complexes for the cooperative catalysis and by the suppression of bimolecular decomposition by immobilization of the complex.[62,63] The catalytic activities of Ru complexes in heterogeneous systems are described together with those in homogeneous systems in Table 1 in order to compare both systems.

The catalytic activity in a [Ru(NH$_3$)$_5$Cl]$^{2+}$/Nafion system[63] was analyzed by considering the contribution of a cooperative catalysis. k_{app} is expressed by eq 4[63] when assuming that the cooperative catalysis can take place within a cooperative catalysis distance, r_{co} (nm).

$$k_{app} = k[\exp\{-4\pi(r_d^3 - s^3)\alpha c N_A \times 10^{-24}/3\} -$$
$$\exp\{-4\pi(r_{co}^3 - s^3)\alpha c N_A \times 10^{-24}/3\}] \quad (4)$$

The best fit of eq 4 to the experimental date was obtained when $k = 2.7 \times 10^{-3}$ s^{-1}, $r_d = 0.84$ nm, and $r_{co} = 1.21$ nm in a [Ru(NH$_3$)$_5$Cl]$^{2+}$/Nafion system.[63] This analysis result indicates that an optimum intermolecular distance exists for the activity. i.e., the intermolecular distance should be between 0.84 and 1.21 nm in the cooperative catalysis by [Ru(NH$_3$)$_5$Cl]$^{2+}$. If water is coordinated directly to the Ru center in the cooperative catalysis, a Ru$-$O$-$O$-$Ru bond (only 0.58 nm from Ru center to center) must be formed as an intermediate. The r_{co} value (1.21 nm) obtained could not be explained by the formation of short Ru$-$O$-$O$-$Ru bond and suggested that a new mechanism for water coordination could be involved, i.e., interaction of water molecule with ammine ligands through hydrogen bonds to form an intermediate such as Ru$-$N$-$H$\cdots$O$-$O$\cdots$H$-$N$-$Ru.[63]

The activity analysis for chemical water oxidation was applied to the other Ru complexes/Nafion systems such as [(NH$_3$)$_5$Ru(μ-O)Ru(NH$_3$)$_5$]$^{4+}$,[60] [(NH$_3$)$_3$Ru(μ-Cl)$_3$Ru(NH$_3$)$_3$]$^{2+}$,[61] [Ru(NH$_3$)$_6$]$^{3+}$,[62] cis-[Ru(NH$_3$)$_4$Cl$_2$]$^+$,[65] and [Ru(en)$_3$]$^{3+}$ (en = ethylenediamine)[64] as well as Ru-red/montmorillonite clay[75] and Ru-red/RuO$_2$ systems,[81] and the parameters k, r_d, and r_{co} (if cooperative catalysis is involved) were obtained. These values were summarized in Table 2, which enabled comparison of water oxidation catalysts in terms of the intrinsic catalytic activity and optimum distance conditions.

B. Electrochemical Water Oxidation

Electrocatalytic water oxidation (Scheme 3) has been investigated using polymer-coated electrodes

Table 2. Summary of Fitting Parameters of the Intrinsic Activity (k), Critical Decomposition Distance (r_d), Cooperative Catalysis Distance (r_{co}), and Contact Distance (s) between the Catalysts in the Nafion Membrane for a Chemical Water Oxidation System Using Ce(IV) Oxidant[a]

system	$k/10^{-3}$ s^{-1}	r_d/nm	r_{co}/nm	s^b/nm	ref
Ru-red	44	1.23		1.06	59
$[(NH_3)_5Ru^{III}(\mu\text{-}O)Ru^{III}(NH_3)_5]^{4+}$	13	1.06		0.98	60
$[(NH_3)_3Ru^{III}(\mu\text{-}Cl)_3Ru^{II}(NH_3)_3]^{2+}$	67	1.22		0.95	61
$[Ru^{III}(NH_3)_6]^{3+}$	0.035	0.82	1.21	0.75	62
$[Ru^{III}(NH_3)_5Cl]^{2+}$	2.7	0.84	1.21	0.75	63
cis-$[Ru^{III}(NH_3)_4Cl_2]^+$	15	0.88		0.75	65
$[Ru^{III}(en)_3]^{3+}$	0.085	1.07	1.44	1.01	64

[a] The α value used in this analysis is 40 (see ref 78). [b] The s value is calculated from the distance and the angle of the atoms as well as the van der Waals radius of hydrogen (see ref 79).
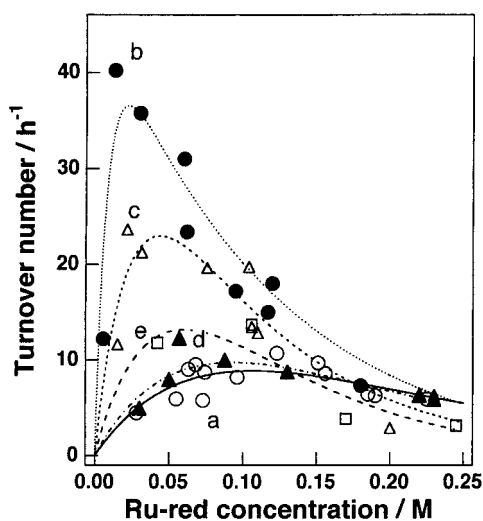

Figure 8. Relationships between the turnover number (TN) of the Ru-red for O₂ evolution and the complex concentration in the membrane in the absence of any amino acid model compound (a) and in the presence of *p*-Cre (b), MIm (c), Tol (d) and Ind (e). (Reprinted with permission from ref 68. Copyright 1998 American Chemical Society.)

containing a molecular catalyst. The catalysts should accept oxidizing equivalents from the electrode and transport them in the membrane by charge hopping between the catalyst molecules, in contrast to the direct charge-transfer reaction from the oxidant to the catalyst in a chemical system. Accordingly, charge transport by charge hopping between the catalysts is a key process for the electrochemical water oxidation catalysis. The intermolecular distance distribution is also an important factor for the charge hopping, and actually charge hopping can be analyzed as a function of a molecular distribution in a matrix.[82] In this section, electrochemical water oxidation catalyzed by a molecular catalyst immobilized in a polymer membrane is reviewed, describing an analysis of the electrocatalytic activity.[66-73]

The electrochemical water oxidation by Ru-red incorporated in Nafion coated on a platinum electrode was reported.[66] The turnover number, TN (h⁻¹), of the Ru-red (corresponding to the activity for O₂ evolution) increased with its concentration under low concentration conditions (Figure 8a), which was interpreted by facilitated charge transfer between the catalysts by hopping. A maximum TN was exhibited, and thereafter it decreased with the concentration. This TN decrease was ascribed to a bimolecular decomposition of the catalyst. TN should be a func-

tion of charge transfer, bimolecular decomposition, and intrinsic activity.[66]

When the charge on the catalysts was assumed to be transferred by hopping between the catalyst molecules present within a charge-transfer distance, r_0 (nm), the TN was given by eq 5[66] on the basis of the intermolecular distance distribution of eq 2

$$TN = k'[\exp\{-4\pi(r_d^3 - s^3)\alpha cN_A \times 10^{-24}/3\} - \exp\{-4\pi(r_0^3 - s^3)\alpha cN_A \times 10^{-24}/3\}] \quad (5)$$

where k'/h^{-1} is a constant to express an intrinsic TN (corresponding to intrinsic activity). The application of eq 5 to the experimental TN data (Figure 8a) results in the best fitting with $k' = 54.8$ h⁻¹, $r_0 = 1.28$ nm, and $r_d = 1.21$ nm.[66] Though the intermolecular distance should be between $r_d = 1.21$ nm and $r_0 = 1.28$ nm to optimize the catalytic activity, the r_d value is close to the r_0 value (see Figure 6), showing that very delicate conditions have to be satisfied for the intermolecular distance between the catalysts in order to establish an efficient and stable electrochemical water oxidation catalyst system. Thus, a difficult problem arises concerning charge transport by hopping between the catalysts in an electrochemical water oxidation system because of the contradictory conditions for the intermolecular distance between the catalysts for the charge transport and bimolecular decomposition, the former requiring a shorter distance and the latter a longer distance. These results reveal that design of molecule-based artificial water oxidation catalysis systems is a difficult problem as long as we stick to a conventional homogeneous or heterogeneous catalyst, compared with the photosynthetic OEC for which the catalysis center is isolated with each other and located in a charge-transfer channel of photosystem II.

The electrocatalytic activity was reported to be enhanced by mediation for charge hopping by amino acid residue model compounds of protein, taking a hint from a long-rang electron transfer observed in biological systems. The electrocatalytic activity of Ru-red in a Nafion membrane was found to increase remarkably by co-dispersing of *p*-cresol (*p*-Cre)[67] (Figure 8b) or 4-methylimidazole (MIm)[68] (Figure 8c), both of which are model compounds of tyrosine or histidine residues. Neither toluene (Tol), model of phenylalanine (Figure 8d), nor 3-methylindole (Ind), model of tryptophan, was effective (Figure 8e). It was concluded that *p*-Cre and MIm work as mediators for

the charge hopping between the catalysts to increase the catalyst activity.

In the presence of the mediator of p-Cre or MIm, it was assumed that the charge on a catalyst molecule is transferred via the mediator to another catalyst molecule present within a mediated charge-transfer distance, r_0' (nm), in addition to direct charge transfer between them present within r_0.

$$\text{TN} = k'[\exp\{-4\pi(r_d{}^3 - s^3)\alpha c N_A \times 10^{-24}/3\} - \\ \exp\{-4\pi(r_0{}^3 - s^3)\alpha c N_A \times 10^{-24}/3\} + \{1 - \\ \exp(-4\pi r_m{}^3 N_A c_m \times 10^{-24}/3)\} \times [\exp\{-4\pi(r_0{}^3 - \\ s^3)\alpha c N_A \times 10^{-24}/3\} - \exp\{-4\pi(r_0'{}^3 - s^3)\alpha c N_A \times \\ 10^{-24}/3\}]] \quad (6)$$

The fit of eq $6^{41,67}$ to the experimental data (Figure 8b,c) showed that the charge-transfer distance was remarkably prolonged from 1.28 to 2.25 nm by the presence of p-Cre[67] and to 1.60 nm by Mim (see Figure 6).[68] The problem of the intermolecular distance (vide supra) was thus overcome by elongating the charge-hopping distance between catalyst molecules by a mediator. These results show that a design of long-range charge transfer between the catalysts is one of the promising approaches to construct an active and stable electrochemical water oxidation catalyst confined in a matrix.

Direct charge injection from the electrode to a molecular catalyst via an electric conducting matrix is also one of the promising approaches to develop the efficient OEC system. It was found that Ru-red is adsorbed on electrodeposited Pt-black particles and works as a highly active catalyst for electrochemical water oxidation.[71,74] The high activity was interpreted by efficient charge transport from the electrode via the Pt-black to Ru-red. Two models were proposed based on the intermolecular distance distribution between the catalysts to analyze the catalytic activity that depends strongly on the amount of the Ru-red adsorbed. One model is a surface adsorption model that assumes adsorption of Ru-red onto the Pt-black particle surface, and the other is a void space adsorption model that assumes adsorption of the catalyst into the void space between the Pt-black particles.[71] These models for activity analysis were also applied to the Ru-red/Au particles,[72] [Ru(NH₃)₅Cl]²⁺/Pt-black,[73] showing a wide application of these models.
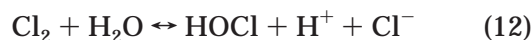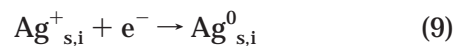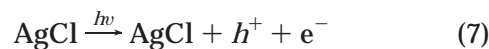
C. Photocatalysts for Water Oxidation

Pt-loaded TiO_2 had been known to decompose water to O_2 and H_2 by UV light irradiation only in the gas phase in the presence of H_2O vapor but not in the liquid phase.[83] It was found by Sayama and Arakawa that addition of carbonate salts to Pt-loaded TiO_2 suspension led to stoichiometric photocatalytic water decomposition to O_2 and H_2 in the liquid phase.[84,85] The presence of a high concentration (1−2 mol dm⁻³) of carbonate ions is essential for this catalysis. They proposed, for a role of carbonate, the O_2 formation mediated by peroxocarbonates such as $C_2O_6{}^{2-}$, $CO_4{}^{2-}$, $HCO_4{}^-$, etc., besides sufficient depression of the back reaction ($2H_2 + O_2 \rightarrow H_2O$) on Pt

and effective desorption of O_2 from a TiO_2 surface to prevent photoadsorption. Namely, the peroxocarbonate species are easily decomposed into O_2 and CO_2 by the holes at a TiO_2 surface, and CO_2 evolution accompanying O_2 evolution might aid the desorption of O_2 from the surface.[85]

Besides TiO_2, it has been reported that heterogeneous photocatalysts such as ZrO_3,[86] $NaTaO_3$,[87] $BaTa_2O_6$,[88] $SrTa_2O_6$,[89] $K_4Nb_6O_{17}$,[90−92] and $K_3TaSi_2O_{13}$[93] can decompose water to evolve O_2 and H_2 without loading any cocatalysts on UV irradiation and that the activities of most of these photocatalysts increased by loading cocatalyst of NiO_x as a proton reduction site. $SrTiO_3$,[94,95] $KTaO_3$,[88,90] Ta_2O_5,[96] Rb_4-Nb_6O_{17},[90] $K_2La_2Ti_3O_{10}$,[97] $Rb_2La_2Ti_3O_{10}$,[97] $Cs_2La_2Ti_3O_{10}$,[97] $CsLa_2Ti_2NbO_{10}$,[97] $Na_2Ti_6O_{13}$,[98] and $BaTi_4O_9$[99] can also evolve O_2 and H_2 with the aid of cocatalysts such as Pt, Rh, NiO_x, and RuO_2. The study on water oxidation by visible light has been carried out using a narrow band-gap photocatalyst. $RbPb_2Nb_3O_{10}$,[100] $BiVO_4$,[101] and $In_2O_3(ZnO)_3$[102] have been reported to be photocatalysts to evolve O_2 from water by visible irradiation in the presence of $AgNO_3$ as a sacrificial electron acceptor.

Calzaferri et al. reported the photocatalytic water oxidation to evolve O_2 at AgCl-coated electrode in an aqueous solution containing a small excess of Ag^+, with a maximum O_2 evolution rate at pH 4−5.[103−105] Electrons are excited from the valence band of semiconductor AgCl to the conduction band by UV light absorption (<380 nm; eq 7). The electron−hole pair may recombine (eq 8) or separate and finally be trapped as reduced silver atoms $Ag^0{}_{s,i}$ at the surface and interstices (eq 9) and as oxidized $Cl^\bullet$ (eq 10). The $Cl^\bullet$ may react with each other to form Cl_2 (eq 11). There is an equilibrium between Cl_2 and $HOCl + Cl^-$ in water (eq 12). The destruction of HOCl was catalyzed by Ag^+ (~10⁻³ M, pH 4−5) to produce O_2 (eq 13). The overall reaction (eq 14) is derived from eqs 7−13. In the AgCl-sensitized systems, Ag^+ works as an electron acceptor to form Ag^0, which is electrochemically reoxidized to Ag^+.

$$\text{AgCl} \xrightarrow{h\nu} \text{AgCl} + h^+ + e^- \quad (7)$$

$$h^+ + e^- \rightarrow \text{recombination} \quad (8)$$

$$\text{Ag}^+{}_{s,i} + e^- \rightarrow \text{Ag}^0{}_{s,i} \quad (9)$$

$$\text{Cl}^-{}_s + h^+ \rightarrow \text{Cl}^\bullet \quad (10)$$

$$2\text{Cl}^\bullet \rightarrow \text{Cl}_2 \quad (11)$$

$$\text{Cl}_2 + \text{H}_2\text{O} \leftrightarrow \text{HOCl} + \text{H}^+ + \text{Cl}^- \quad (12)$$

$$2\text{HOCl} \xrightarrow{\text{Ag}^+} \text{O}_2 + 2\text{H}^+ + 2\text{Cl}^- \quad (13)$$

$$\text{H}_2\text{O} + \text{Ag}^+ \xrightarrow{h\nu,\text{ AgCl}} 2\text{H}^+ + {}^1\!/_2\text{O}_2 + 2\text{Ag}^0 \quad (14)$$

Domen et al. reported a new concept, mechanocatalysis for water splitting, in which the aqueous metal oxide such as NiO, Co_3O_4, Cu_2O, Fe_3O_4, and $CuMO_2$ (M = Al, Fe, Ga), when suspended in distilled water by magnetic stirring, decomposes water into H_2 and O_2.[106,107] They demonstrated that the O_2 and

H$_2$ evolution rates increased with increasing the revolution rate of the rotating rod and also depended on the shape of the rod, indicating that this reaction was driven by the mechanical energy consumed at the interface between the rotating rod and the bottom of the reaction vessel. Although they suggested the participation of reduced metallic Cu, Ni, and Co to produce H$_2$ during the mechano-catalytic reaction on Cu$_2$O, NiO, and Co$_3$O$_4$, the contributing mechanism of mechano-catalysis for water decomposition, particularly O$_2$ evolution, is unresolved. Interestingly, the catalytic activity of the mechano-catalysis at Cu$_2$O was improved by visible light irradiation.[106,108] The mechanism of this improvement, e.g., whether photoenergy conversion or acceleration of the mechano-catalysis by visible light, also remains open.

V. Design of Artificial Photosystem II (PS II) Model

The construction of an artificial PS II in which visible light induces water oxidation to evolve O$_2$ has been attracting attention since this reaction is an important and essential part of photochemical solar energy conversion in an artificial photosynthetic system. However, it has been difficult to establish a PS II model because of the difficulty to couple four-electron transfer for water oxidation with one-electron excitation at the photosensitizer. Recent examples of approaches to an artificial PS II model will be reviewed here.

Sun et al. reported tris(bipyridine)ruthenium(II) complex covalently linked to a manganese(II) complex as a first step of mimicking PS II and showed that after initial electron transfer from the photoexcited Ru(II) to an external electron acceptor, methyl viologen (MV^{2+}), intramolecular electron transfer takes place from the Mn(II) to the photogenerated Ru(III) in acetonitrile solution[109−112] (Figure 9). They also reported tris(bipyridine)ruthenium(II) covalently attached to tyrosyl moiety to show that a tyrosyl radical is formed by intramolecular electron transfer from the tyrosyl moiety to a photogenerated Ru(III) in the presence of Co(NH$_3$)$_5$Cl^{2+} or sodium persulfate working as an external sacrificial electron acceptor in aqueous and acetonitrile solutions.[111] The rate constant of the intramolecular electron transfer increased by 2 orders of magnitude by the aid of the dipicolylamine arm linked to tyrosyl moiety.[113] The hydrogen bonds between tyrosyl moiety and dipicolylamine arm were suggested to be responsible for the enhanced electron transfer, and this interaction was considered as a mimic of the proposed His 190 and Tyr$_z$ interaction in PS II. Subsequently, they showed that external dinuclear manganese complex could be oxidized by the tyrosyl radical photogenerated by the intramolecular electron transfer in the aqueous solution[114] and further that manganese dimer covalently linked to Ru photosensitizer via a tyrosine unit could be oxidized by photogenerated Ru-(III).[115]

Similar approaches to these works were reported by Burdinski et al., in which mono-, di-, and trinuclear manganese complexes with phenolate ligands covalently linked to tris(bipyridine)ruthenium(II)
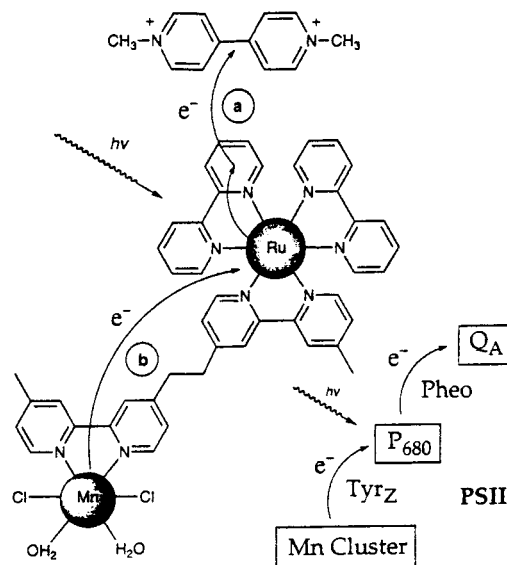

Figure 9. Photoinduced electron transfer in the Ru−Mn binuclear complex. (Reprinted with permission from ref 109. Copyright 1997 American Chemical Society.)

were synthesized and characterized.[116] They showed that intramolecular electron transfer takes place from a Mn^{II}-trimer moiety to the photochemically generated Ru(III) as well as from a phenolate ligand to the Ru(III) in a Mn^{IV}-monomer derivative.[117] These works by Sun et al. and Burdinski et al. may offer mechanistic insight into elucidation of electron-transfer coupled with proton transfer proposed to be involved in photosynthetic water oxidation. However, O$_2$ is not produced from water in the present stage of their projects. These type of approaches, i.e., water oxidation catalyst covalently linked to photosensitizer such as tris(bipyridine)ruthenium(II), might be possible to establish a photochemical water oxidation with assistance of a sacrificial electron acceptor like Co(NH$_3$)$_5$Cl^{2+}, if a highly active catalyst could be developed.

O$_2$ evolution from water was induced by visible light at a mutilayer-modified electrode composed of a Nafion membrane incorporating Ru(bpy)$_3$$^{2+}$ sensitizer and electrodeposited platinum-black adsorbing Ru-red.[118] Elsewhere, the visible-light excitation of 1,2,3,4,5,6,7,8-octafluorophenazine in the presence of water in acetonitrile was found to participate in one-electron oxidation of water to hydroxy radical to produce stoichiometrically 2-hydroxyphenazine derivative.[119]

Water splitting by semiconductor has been also studied. It was reported by Khaselev and Turner that water electrolysis to O$_2$ and H$_2$ is achieved upon white light illumination under the short-circuit conditions at monolithic photovoltaic−photoelectrochemical tandem cell device, which consists of a GaAs bottom cell connected to a GaInP$_2$ top cell through a tunnel diode interconnect (Figure 10).[120] This might be one of the candidates for an approach to construct an efficient artificial photosynthetic system.

VI. Conclusion and Future Scopes

For water oxidation in the OEC, mechanisms involving manganyl (Mn=O) species as an intermedi-
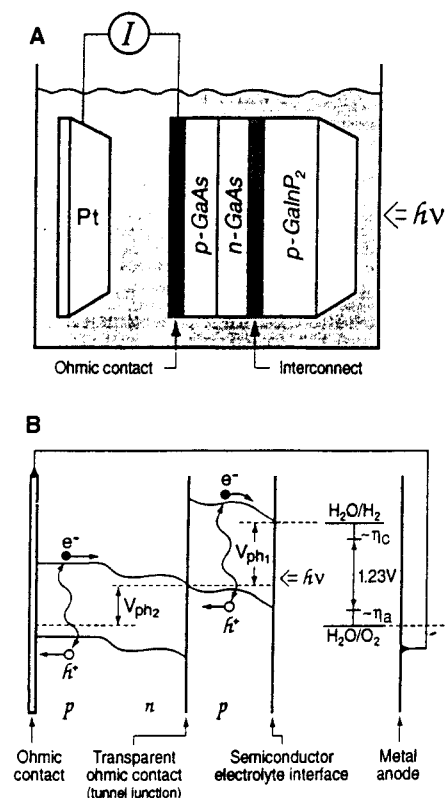
Figure 10. Schematic (A) and ideal energy-level diagram (B) for the monolithic photovoltaic−photoelectrochemical tandem cell device. (Reprinted with permission from ref 120. Copyright 1998 American Association for the Advancement of Science.)

ate with minimal structural core changes or with redox reaction of only one Mn atom have been recently proposed besides previous mechanisms involving structural conversions from Mn_4O_4 cubane core to Mn_4O_6 adamantane core and from Mn_4O_2 butterfly core to Mn_4O_4 cubane core. Water oxidation by manganese model complexes has been reported to reveal the mechanism involving Mn=O for water oxidation in the OEC, but the reaction mechanism including the source of oxygen atom for O_2 production is unclear. O_2 production from a Mn_4O_4 cubane core structure has been reported, indicating that the structural conversion from Mn_4O_2 butterfly core to Mn_4O_4 cubane core cannot be excluded. To conclude, any proposed mechanisms of water oxidation in the OEC are not sufficiently corroborated in the present time.

Di- and tetranuclear manganese complexes as well as mono-, di-, and trinuclear ruthenium complexes have been reported as molecular catalysts capable of evolving O_2 from water. Ammine-coordinated multinuclear Ru complexes are more active than mononuclear ruthenium and manganese complexes. Irrespective of manganese and ruthenium complexes, a multinuclear structure would be important to develop active and stable catalysts. This would be because multinuclear structure can accumulate and delocalize four oxidizing equivalents. This would also lead to insight into photosynthetic OEC composed of tetramanganese oxo cluster.

A contribution of chloride or hypochlorite ion to water oxidation catalysis by synthetic molecular catalysts has been reported in the several works. Despite no obvious corroboration of the roles, water oxidation catalysis coupled with the redox chemistry of chloride or hypochlorite ion might provide a new concept for the development of the active molecular catalysts. The contribution of chloride ion is also interesting when compared with catalysis in the photosynthetic OEC in which chloride ion is necessary to its photoactivation, though its role may be different in both biological and artificial systems.

Intermolecular decomposition of complex catalysts involving oxidation of their organic ligands, which is thermodynamically easier than water oxidation, is an essential problem for water oxidation by complex catalysts. Elaborated design and synthesis to prohibit the intermolecular decomposition is one of the possible approaches to stabilize molecular catalysts. It has been demonstrated that immobilization of the molecular catalysts onto heterogeneous matrixes prohibits dynamic intermolecular decomposition without loss of catalytic activity.

In the electrochemical water oxidation system, the problem is encountered in the charge transport from an electrode to catalyst molecules. Namely, the shorter intermolecular distance is better for charge transport, but longer is better for the stabilization against intermolecular decomposition. This implies that it would be difficult to design the OEC model under convergent conditions, irrespective of homogeneous and heterogeneous systems, as long as the catalyst molecule is not designed on a molecular level like a photosynthetic OEC. A new concept of a charge-hopping mediator has been proposed to overcome the problem of intermolecular distance besides utilization of an electric conductive matrix to accomplish direct charge injection from an electrode to catalyst molecules.

It had been difficult to compare the intrinsic activity and optimum conditions of molecular catalysts since any models to analyze molecular aspects of catalysts did not exist. Analysis models were proposed considering intermolecular interaction of the catalysts which affect the activity in heterogeneous matrixes.

An efficient PS II model has not been established so far. Construction of an efficient PS II would be an important subject for the 21st century in addition to development of more active and stable OEC model systems. This would lead not only to a first step for creating a renewable energy source with no emission, but also to insight into the photosynthetic PS II.

VII. Acknowledgments

dation and Science, and Technology Foundation of Siseido.

VIII. References

(1) Hall, D. O.; Krishna, R. In *Photosynthesis* 6th; Cambridge University Press: 1999.
(2) Kaneko, M. *11th Symposium on Unsolved Problems in Polymer Science*; The Society of Polymer Science: Japan, 1976; p 21.
(3) Kaneko, M. In *Macromolecular Complexes: Dynamic Interaction and Electronic Processes*; Tsuchida, E., Ed.; VCH Publishers: New York, 1991.
(4) Kaneko, M. In *Organic Conductive Molecules and Polymers*; Nalwa, H. S., Ed.; John Wiley & Sons: Ltd.: Chichester, 1997; Vol. 4.
(5) Ramaraj, R.; Kaneko, M. In *Advances in Polymer Science*; Springer-Verlag: Berlin, 1995; Vol. 123.
(6) Ruettinger, W.; Dismukes, G. C. *Chem. Rev.* **1997**, *97*, 1−24.
(7) Manchanda, R.; Brudvig, G. W.; Crabtree, R. H. *Coord. Chem. Rev.* **1995**, *144*, 1−38.
(8) Pecoraro, V. L.; Baldwin, M. J.; Gelasco, A. *Chem. Rev.* **1994**, *94*, 807−826.
(9) Law, N. A.; Caudle, M. T.; Pecoraro, V. L. In *Advances in Inorganic Chemistry*; Academic Press Inc.: San Diego, 1999; Vol. 46.
(10) Meyer, T. J. *Acc. Chem. Res.* **1989**, *22*, 163−170.
(11) Bard, A. J.; Fox, M. A. *Acc. Chem. Res.* **1995**, *28*, 141−145.
(12) Graetzel, M.; Kalyanasundaram, K. *Curr. Sci.* **1994**, *66*, 706−714.
(13) Dismukes, G. C.; Siderer, Y. *Proc. Natl. Acad. Sci., U.S.A.* **1981**, *78*, 274−278.
(14) Dismukes, G. C.; Ferris, K.; Watnick, P. *Photobiochem. Photobiophys.* **1982**, *3*, 243−256.
(15) Kok, B.; Forbush, B.; McGloin, M. P. *Photochem. Photobiol.* **1970**, *11*, 457−475.
(16) Yachandra, V. K.; Sauer, K.; Klein, M. P. *Chem. Rev.* **1996**, *96*, 2927−2950.
(17) Debus, R. J. *Biochim. Biophys. Acta* **1992**, *1102*, 269−352.
(18) Britt, R. D. In *Oxgenic Photosynthesis: The Light Reaction*; Ort, D. R., Yocum, C. F., Eds.; Kluwer Academic Publishers: Dordrecht, 1996.
(19) Hoganson, C. W.; Babcock, G. T. *Science* **1997**, *277*, 1953−1956.
(20) Dismukes, G. C.; Ruettinger, W.; Boelrijk, A. E. M.; Ho, D. In *Proceedings XIth International Photosynthesis Congress*; Garab, G., Ed.; Kluwer Academic: Dordrecht, 1998; Vol. II.
(21) Brudvig, G. W.; Crabtree, R. H. *Proc. Natl. Acad. Sci. U.S.A.* **1986**, *83*, 4586−4588.
(22) Vincent, J. B.; Christou, G. *Inorg. Chim. Acta* **1987**, *136*, L41−L43.
(23) Hoganson, C. W.; Babcock, G. T. In *Metals in Biology Series*; Sigel, H., Sigel, A., Eds., 2000; Vol. 37.
(24) Tommos, C.; Hoganson, C. W.; Di Valentin, M.; Lydakis-Simantiris, N.; Dorlet, P.; Westphal, K.; Chu, H. A.; McCracken, J.; Babcock, G. T. *Curr. Opin. Chem. Biol.* **1998**, *2*, 244−252.
(25) Tommos, C.; Babcock, G. T. *Acc. Chem. Res.* **1998**, *31*, 18−25.
(26) Limburg, J.; Szalai, V. A.; Brudvig, G. W. *J. Chem. Soc., Dalton Trans.* **1999**, 1353−1361.
(27) Siegbahn, P. E. M.; Crabtree, R. H. *J. Am. Chem. Soc.* **1999**, *121*, 117−127.
(28) Casey, J. L.; Sauer, K. *Biochim. Biophys. Acta* **1984**, *767*, 21−28.
(29) Zimmermann, J.-L.; Rutherford, A. W. *Biochim. Biophys. Acta* **1984**, *767*, 7507−7511.
(30) Randall, D. W.; Sturgeon, B. E.; Ball, J. A.; Lorigan, G. A.; Chan, M. K.; Klein, M. P.; Armstrong, W. H.; Britt, R. D. *J. Am. Chem. Soc.* **1995**, *117*, 11780−11789.
(31) Ono, T.; Noguchi, T.; Inoue, Y.; Kusunoki, M.; Matsushita, T.; Oyanagi, H. *Science* **1992**, *258*, 1335−1337.
(32) Hundelt, M.; Haumann, M.; Junge, W. *Biochim. Biophys. Acta* **1997**, *1321*, 47−60.
(33) Baldwin, M. J.; Gelasco, A.; Pecoraro, V. L. *Photosynth. Res.* **1993**, *38*, 303−308.
(34) Sivaraja, M.; Tso, J.; Dismukes, G. C. *Biochemistry* **1989**, *28*, 9459−9464.
(35) Pecoraro, V. L.; Baldwin, M. J.; Caudle, M. T.; Hsieh, W. Y.; Law, N. A. *Pure Appl. Chem.* **1998**, *70*, 925−929.
(36) Yamada, H.; Hurst, J. K. *J. Am. Chem. Soc.* **2000**, *122*, 5303−5311.
(37) Feichtinger, D.; Plattner, D. A. *Angew. Chem., Int. Ed. Engl.* **1997**, *36*, 1718−1719.
(38) Siegbahn, P. E. M. *Inorg. Chem.* **2000**, *39*, 2923−2935.
(39) Rhee, K. H.; Morriss, E. P.; Barber, J.; Kuhlbrandt, W. *Nature* **1998**, *396*, 283−286.
(40) Zouni, A.; Jordan, R.; Schlodder, E.; Fromme, P.; Witt, H. T. *Biochim. Biophys. Acta, Bioenerg.* **2000**, *1457*, 103−105.
(41) Witt, H. T. The 13th international conference on photochemical conversion and storage of solar energy (IPS-2000), Snowmass, CO, 2000; p V-7.
(42) Ramaraj, R.; Kira, A.; Kaneko, M. *Angew. Chem., Int. Ed. Engl.* **1986**, *25*, 825−827.
(43) Naruta, Y.; Sasayama, M.; Sasaki, T. *Angew. Chem., Int. Ed. Engl.* **1994**, *33*, 1839−1841.
(44) Limburg, J.; Brudvig, G. W.; Crabtree, R. H. *J. Am. Chem. Soc.* **1997**, *119*, 2761−2762.
(45) Limburg, J.; Vrettos, J. S.; Liable-Sands, L. M.; Rheingold, A. L.; Crabtree, R. H.; Brudvig, G. W. *Science* **1999**, *283*, 1524−1527.
(46) Collomb, M. N.; Deronzier, A.; Richardot, A.; Pecaut, J. *New J. Chem.* **1999**, *23*, 351−353.
(47) Brudvig, G. W.; Crabtree, R. H. Personal communication, 1999.
(48) Lister, M. W.; Petterson, R. C. *Can. J. Chem.* **1962**, *40*, 729.
(49) Ruettinger, W. F.; Campana, C.; Dismukes, G. C. *J. Am. Chem. Soc.* **1997**, *119*, 6670−6671.
(50) Ruettinger, W. F.; Ho, D. M.; Dismukes, G. C. *Inorg. Chem.* **1999**, *38*, 1036−1037.
(51) Ruettinger, W.; Dismukes, G. C. *Inorg. Chem.* **2000**, *39*, 1021−1027.
(52) Ruettinger, W.; Yagi, M.; K. Wolf; Bernasek, S.; Dismukes, G. C. *J. Am. Chem. Soc.* **2000**, in press.
(53) Dube, C. E.; Wright, D. W.; Pal, S.; Bonitatebus, P. J.; Armstrong, W. H. *J. Am. Chem. Soc.* **1998**, *120*, 3704−3716.
(54) Dunand-Sauthier, M. N. C.; Deronzier, A.; Piron, A.; Pradon, X.; Menage, S. *J. Am. Chem. Soc.* **1998**, *120*, 5373−5380.
(55) Gorun, S. M.; Stibrany, R. T.; Lillo, A. *Inorg. Chem.* **1998**, *37*, 836−837.
(56) For example, references in ref 6.
(57) Chronister, C. W.; Binstead, R. A.; Ni, J. F.; Meyer, T. J. *Inorg. Chem.* **1997**, *36*, 3814−3815.
(58) Lebeau, E. L.; Adeyemi, S. A.; Meyer, T. J. *Inorg. Chem.* **1998**, *37*, 6476−6484.
(59) Yagi, M.; Tokita, S.; Nagoshi, K.; Ogino, I.; Kaneko, M. *J. Chem. Soc., Faraday Trans.* **1996**, *92*, 2457−2461.
(60) Nagoshi, K.; Yagi, M.; Kaneko, M. *Bull. Chem. Soc. Jpn.* **2000**, in press.
(61) Yagi, M.; Osawa, Y.; Sukegawa, N.; Kaneko, M. *Langmuir* **1999**, *15*, 7406−7408.
(62) Yagi, M.; Sukegawa, N.; Kasamastu, M.; Kaneko, M. *J. Phys. Chem. B* **1999**, *103*, 2151−2154.
(63) Yagi, M.; Nagoshi, K.; Kaneko, M. *J. Phys. Chem. B* **1997**, *101*, 5143−5146.
(64) Yagi, M.; Kasamastu, M.; Kaneko, M. *J. Mol. Catal. A, Chem.* **2000**, *151*, 29−35.
(65) Yagi, M.; Sukegawa, N.; Kaneko, M. *J. Phys. Chem. B* **2000**, *104*, 4111−4114.
(66) Yagi, M.; Kinoshita, K.; Kaneko, M. *J. Phys. Chem.* **1996**, *100*, 11098−11100.
(67) Yagi, M.; Kinoshita, K.; Kaneko, M. *J. Phys. Chem. B* **1997**, *101*, 3957−3960.
(68) Kinoshita, K.; Yagi, M.; Kaneko, M. *Macromolecules* **1998**, *31*, 6042−6045.
(69) Kinoshita, K.; Yagi, M.; Kaneko, M. *J. Mol. Catal. A, Chem.* **1999**, *142*, 1−5.
(70) Shiroishi, H.; Yamashita, S.; Kinoshita, K.; Kaneko, M. *Polym. J.* **1999**, *31*, 1175−1178.
(71) Ogino, O.; Nagoshi, K.; Yagi, M.; Kaneko, M. *J. Chem. Soc., Faraday Trans.* **1996**, *92*, 3431−3434.
(72) Yagi, M.; Takano, E.; Kaneko, M. *Electrochim. Acta* **1999**, *44*, 2493−2497.
(73) Yagi, M.; Yamaguchi, T.; Kaneko, M. *J. Mol. Catal. A: Chem.* **1999**, *149*, 289−295.
(74) Yagi, M.; Ogino, I.; Miura, A.; Kurimura, Y.; Kaneko, M. *Chem. Lett.* **1995**, 863−864.
(75) Yamashita, S.; Nagoshi, K.; Yagi, M.; Kaneko, M. *J. Mol. Catal. A, Chem.* **2000**, *153*, 209−214.
(76) Nagoshi, K.; Yamashita, S.; Yagi, M.; Kaneko, M. *J. Mol. Catal. A, Chem.* **1999**, *144*, 71−76.
(77) The initial O_2 evolution rate is obtained from the initial slope of the amount of O_2 vs time plots, giving an approximately liner relationship up to 30 min (ref 59).
(78) The value of α is calculated from the fraction of its hydrophilic column. An α value of 40 (ref 59) was used for a commercially available Nafion membrane in chemical water oxidation and 5.1 (ref 66) for a cast-membrane formed from a Nafion solution in electrochemical water oxidation.
(79) s is the sum of van der Waals radii of a catalyst, calculated from the distance and the angle of the atoms as well as the van der Waals radius of hydrogen. (see refs 59 and 63).
(80) The r_d, obtained in the activity analysis on molecular distribution, includes contributions from the segmental motion of polymer and the bounded motion of the complex (local oscillation) (see ref 82). However, it could be assumed that despite these factors, the distribution of the dispersed molecules would maintain a random one at every moment, so that these motions would not affect the distribution of the complex as a whole. The

positive charges on the complex would be compensated by the sulfonate anions of Nafion. We assume also that the distribution has a random distribution even if the interaction between the positive charges on the complexes is not negligible, since an isotropic perturbation by the charges would cause a random distribution in the membrane.

(81) Abe, T.; Tamada, Y.; Shiroishi, H.; Nukaga, M.; Kaneko, M. *J. Mol. Catal. A, Chem.* **1999**, *144*, 389−395.
(82) Yagi, M.; Nagai, K.; Onikubo, T.; Kaneko, M. *J. Electroanal. Chem.* **1995**, *383*, 61−66.
(83) Sato, S.; White, J. M. *Chem. Phys. Lett.* **1980**, *72*, 83.
(84) Sayama, K.; Arakawa, H. *J. Chem. Soc., Chem. Commun.* **1992**, 150−152.
(85) Sayama, K.; Arakawa, H. *J. Chem. Soc., Faraday Trans.* **1997**, *93*, 1647−1654.
(86) Sayama, K.; Arakawa, H. *J. Phys. Chem.* **1993**, *97*, 531−533.
(87) Kato, H.; Kudo, A. *Catal. Lett.* **1999**, *58*, 153−155.
(88) Kato, H.; Kudo, A. *Chem. Phys. Lett.* **1998**, *295*, 487−492.
(89) Kato, H.; Kudo, A. *Chem. Lett.* **1999**, 1207−1208.
(90) Sayama, K.; Arakawa, H.; Domen, K. *Catal. Today* **1996**, *28*, 175−182.
(91) Sayama, K.; Yase, K.; Arakawa, H.; Asakura, K.; Tanaka, A.; Domen, K.; Onishi, T. *J. Photochem. Photobiol. A, Chem.* **1998**, *114*, 125−135.
(92) Ikeda, S.; Tanaka, A.; Shinohara, K.; Hara, M.; Kondo, J. N.; Maruya, K. I.; Domen, K. *Microporous Mater.* **1997**, *9*, 253−258.
(93) Kudo, A.; Kato, H. *Chem. Lett.* **1997**, 867−868.
(94) Lehn, J.-M.; Sauvage, J.-P.; Ziessel, R. *Nouv. J. Chim.* **1980**, *4*, 623.
(95) Domen, K.; Kudo, A.; Ohnishi, T. *J. Catal.* **1986**, *102*, 92.
(96) Sayama, K.; Arakawa, H. *J. Photochem. Photobiol. A, Chem.* **1994**, *77*, 243−247.
(97) Takata, T.; Furumi, Y.; Shinohara, K.; Tanaka, A.; Hara, M.; Kondo, J. N.; Domen, K. *Chem. Mater.* **1997**, *9*, 1063−1064.
(98) Inoue, Y.; Kubokawa, T.; Sato, K. *J. Phys. Chem.* **1991**, *95*, 4059−4063.
(99) Kohno, M.; Kaneko, T.; Ogura, S.; Sato, K.; Inoue, Y. *J. Chem. Soc., Faraday Trans.* **1998**, *94*, 89−94.
(100) Yoshimura, J.; Ebina, Y.; Kondo, J.; Domen, K.; Tanaka, A. *J. Phys. Chem.* **1993**, *97*, 1970−1973.
(101) Kudo, A.; Ueda, K.; Kato, H.; Mikami, I. *Catal. Lett.* **1998**, *53*, 229−230.
(102) Kudo, A.; Mikami, I. *Chem. Lett.* **1998**, 1027−1028.
(103) Lanz, M.; Schurch, D.; Calzaferri, G. *J. Photochem. Photobiol. A: Chem.* **1999**, *120*, 105−117.
(104) Pfanner, K.; Gfeller, N.; Calzaferri, G. *J. Photochem. Photobiol. A: Chem.* **1996**, *95*, 175−180.
(105) Saladin, F.; Kamber, I.; Pfanner, K.; Calzaferri, G. *J. Photochem. Photobiol. A: Chem.* **1997**, *109*, 47−52.
(106) Ikeda, S.; Takata, T.; Kondo, T.; Hitoki, G.; Hara, M.; Kondo, J. N.; Domen, K.; Hosono, H.; Kawazoe, H.; Tanaka, A. *Chem. Commun.* **1998**, 2185−2186.
(107) Ikeda, S.; Takata, T.; Komoda, M.; Hara, M.; Kondo, J. N.; Domen, K.; Tanaka, A.; Hosono, H.; Kawazoe, H. *Phys. Chem. Chem. Phys.* **1999**, *1*, 4485−4491.
(108) Hara, M.; Kondo, T.; Komoda, M.; Ikeda, S.; Shinohara, K.; Tanaka, A.; Kondo, J. N.; Domen, K. *Chem. Commun.* **1998**, 357−358.
(109) Sun, L. C.; Berglund, H.; Davydov, R.; Norrby, T.; Hammarstrom, L.; Korall, P.; Borje, A.; Philouze, C.; Berg, K.; Tran, A.; Andersson, M.; Stenhagen, G.; Martensson, J.; Almgren, M.; Styring, S.; Akermark, B. *J. Am. Chem. Soc.* **1997**, *119*, 6996−7004.
(110) Sun, L. C.; Hammarstrom, L.; Norrby, T.; Berglund, H.; Davydov, R.; Andersson, M.; Borje, A.; Korall, P.; Philouze, C.; Almgren, M.; Styring, S.; Akermark, B. *Chem. Commun.* **1997**, 607−608.
(111) Magnuson, A.; Berglund, H.; Korall, P.; Hammarstrom, L.; Akermark, B.; Styring, S.; Sun, L. C. *J. Am. Chem. Soc.* **1997**, *119*, 10720−10725.
(112) Berglund-Baudin, H.; Sun, L. C.; Davidov, R.; Sundahl, M.; Styring, S.; Akermark, B.; Almgren, M.; Hammarstrom, L. *J. Phys. Chem. A* **1998**, *102*, 2512−2518.
(113) Sun, L. C.; Burkitt, M.; Tamm, M.; Raymond, M. K.; Abrahamsson, M.; LeGourrierec, D.; Frapart, Y.; Magnuson, A.; Kenez, P. H.; Brandt, P.; Tran, A.; Hammarstrom, L.; Styring, S.; Akermark, B. *J. Am. Chem. Soc.* **1999**, *121*, 6834−6842.
(114) Magnuson, A.; Frapart, Y.; Abrahamsson, M.; Horner, O.; Akermark, B.; Sun, L. C.; Girerd, J. J.; Hammarstrom, L.; Styring, S. *J. Am. Chem. Soc.* **1999**, *121*, 89−96.
(115) Sun, L. C.; Raymond, M. K.; Magnuson, A.; LeGourrierec, D.; Tamm, M.; Abrahamsson, M.; Kenez, P. H.; Martensson, J.; Stenhagen, G.; Hammarstrom, L.; Styring, S.; Akermark, B. *J. Inorg. Biochem.* **2000**, *78*, 15−22.
(116) Burdinski, D.; Bothe, E.; Wieghardt, K. *Inorg. Chem.* **2000**, *39*, 105−116.
(117) Burdinski, D.; Wieghardt, K.; Steenken, S. *J. Am. Chem. Soc.* **1999**, *121*, 10781−10787.
(118) Yagi, M.; Takahashi, Y.; Ogino, I.; Kaneko, M. *J. Chem. Soc., Faraday Trans.* **1997**, *93*, 3125−3127.
(119) Kitamura, T.; Fudemoto, H.; Wada, Y.; Murakoshi, K.; Kusaba, M.; Nakashima, N.; Majima, T.; Yanagida, S. *J. Chem. Soc., Faraday Trans.* **1997**, *93*, 221−229.
(120) Khaselev, O.; Turner, J. A. *Science* **1998**, *280*, 425−427.